

HOSTED BY



ELSEVIER

Contents lists available at ScienceDirect

Egyptian Journal of Petroleum

journal homepage: www.sciencedirect.com



Full Length Article

Organic geochemistry characterisation of crude oils from Mishrif reservoir rocks in the southern Mesopotamian Basin, South Iraq: Implication for source input and paleoenvironmental conditions

Amer Jassin Al-Khafaji^a, Mohammed Hail Hakimi^{b,*}, Ahmed Askar Najaf^c

^a Department of Geology, University of Babylon, Al Hillah, Iraq

^b Geology Department, Faculty of Applied Science, Taiz University, 6803 Taiz, Yemen

^c College of Geophysics and Remote Sensing, Al-Karkh University, Iraq

ARTICLE INFO

Article history:

Received 13 December 2016

Accepted 5 February 2017

Available online xxxxx

Keywords:

Crude oil

Biomarker

Carbon isotope

Depositional environment

Source inputs

Type II-S

Mesopotamian Basin, South Iraq

ABSTRACT

Seven crude oils from Cretaceous Mishrif reservoir rocks in the southern Mesopotamian Basin, South Iraq were studied to describe oil characteristics, providing information on the source of organic matter input and the genetic link between oils and their potential source rock in the basin. This study is based on biomarker and non-biomarker analyses performed on oil samples. The analysed oils are aromatic intermediate oils as indicated by high aromatic hydrocarbon fractions with more than 50%. These oils are also characterized by high sulfur and trace metal (Ni, V) contents and relatively low API gravity values (19.0–27.2° API). The results of this study indicate that these oils were derived from a marine carbonate source rocks bearing Type II-S kerogen that were deposited under sulphate-reducing conditions. This is primarily achieved from their biomarkers and bulk carbon isotope and inorganic element contents (i.e., S, Ni and V). The absence of 18a (H)-oleanane biomarker also suggests a source age older than Late Cretaceous. The biomarker characteristics of these oils are consistent with those of the Late Jurassic to Early Cretaceous source rocks in the basin. However, biomarker maturity data also indicate that the oils were generated from early maturity source rocks. This appears to result from the type of kerogen of the source rock, characterized by a high-S kerogen (Type II-S).

© 2017 Egyptian Petroleum Research Institute. Production and hosting by Elsevier B.V. This is an open access article under the CC BY-NC-ND license (<http://creativecommons.org/licenses/by-nc-nd/4.0/>).

1. Introduction

Mesopotamian basin is one of the main basins in Iraq, which is extended from north to south Iraq (Fig. 1a). Mesopotamian Basin is considered as one of the richest petroleum systems in the world [1–3]. The Mesopotamian Basin is an important hydrocarbon province in Iraq and contains several, well known oil fields (Fig. 1a). The dataset used herein is from the oil field, which are located in the southern part of the Mesopotamian Basin (Fig. 1b). The Mesopotamian Basin has attracted the interest of numerous researchers and oil companies. Several studies have been undertaken on the potential source rocks in the basin [4–6]. The presence of possible source rocks in the Mesopotamian Basin is Late Jurassic to Cretaceous units, which are including Sulaiy (Late Jurassic), Yamama and Ratawi (Early Cretaceous) and Zubair (Middle Cretaceous) Formations [5,6]. Abeed et al. [6] concluded that the best quality

source rocks in the southern Mesopotamian Basin are the Late Jurassic–Early Cretaceous marine carbonates (Sulaiy Formation and possibly also Yamama Formation). They are bituminite limestones and black shales, which have high organic matter (TOC) with more than 3 wt% [6]. These source rocks were deposited in a carbonate-rich, anoxic environment and favoured by salinity stratification [6]. The Sulaiy and Yamama source rocks have also high sulfur contents (>3 wt%) [6], suggest the presence of kerogen Type II-S, and thus have to be generated early-mature sulfur-rich oils. However, the quality of crude oils and the origin of organic matter input and depositional environment conditions of their potential source rocks in the Mesopotamian Basin are limited. The main objectives of the current study were to: (1) characterize the oil types and compositions in the southern Mesopotamian Basin, South Iraq; (2) to provide insight into the source organic matter input, palaeo-depositional conditions, and thermal maturity of the respective their source rocks. In this study, seven (7) crude oils from Early Cretaceous Mishrif petroleum reservoir rock in the three oilfields (i.e., West Qurna, Zubair, and Nasriah), Southern Mesopotamian Basin (Fig. 1b) were analysed by a variety of geochemical techniques.

Peer review under responsibility of Egyptian Petroleum Research Institute.

* Corresponding author.

E-mail address: ibnalhakimi@yahoo.com (M.H. Hakimi).

<http://dx.doi.org/10.1016/j.ejpe.2017.02.001>

1110-0621/© 2017 Egyptian Petroleum Research Institute. Production and hosting by Elsevier B.V.

This is an open access article under the CC BY-NC-ND license (<http://creativecommons.org/licenses/by-nc-nd/4.0/>).

Please cite this article in press as: A.J. Al-Khafaji et al., Organic geochemistry characterisation of crude oils from Mishrif reservoir rocks in the southern Mesopotamian Basin, South Iraq: Implication for source input and paleoenvironmental conditions, Egypt. J. Petrol. (2017), <http://dx.doi.org/10.1016/j.ejpe.2017.02.001>

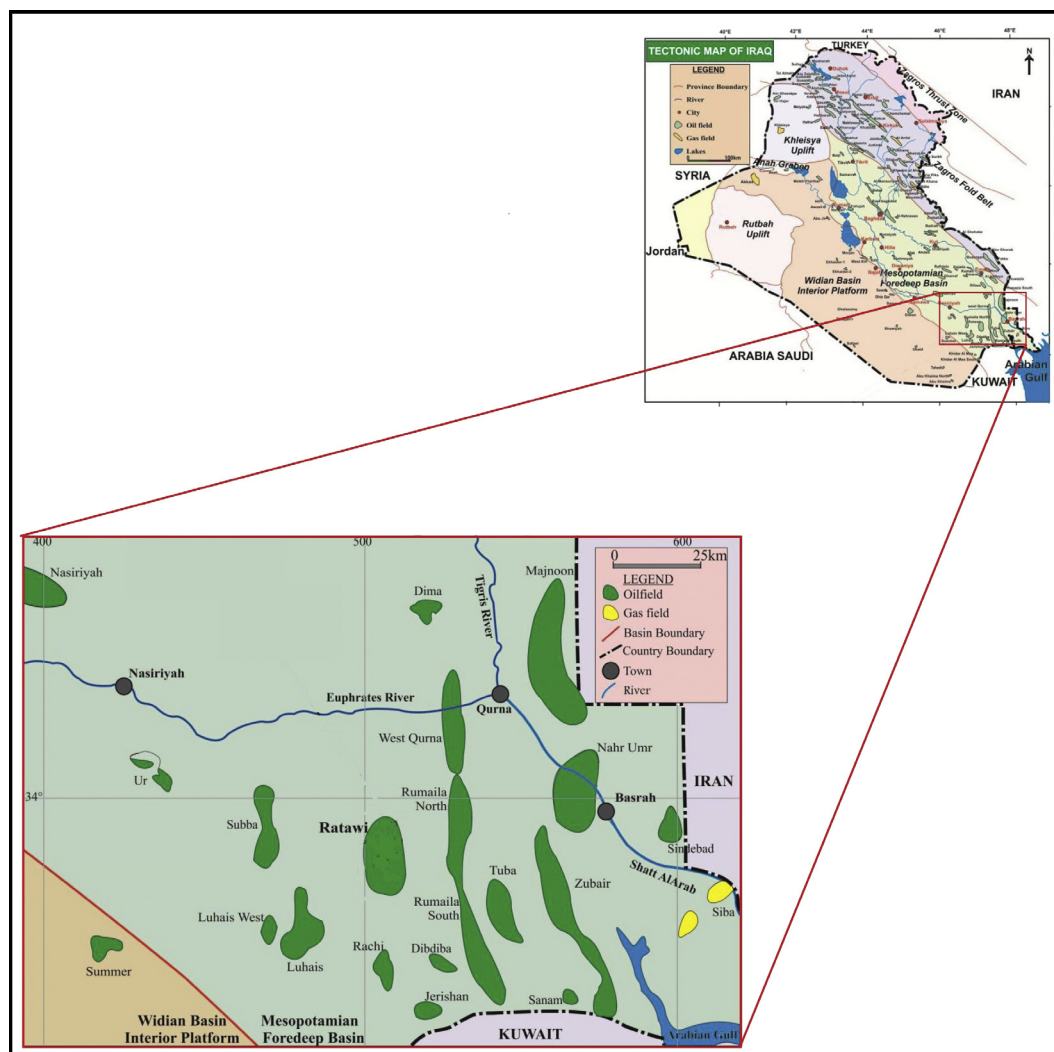


Fig. 1. Location map for the northeast Arabian Peninsula in Iraq, which shows Mesopotamian and Zagross Fold Belt basins with oil and gas field locations, including study oilfield locations.

2. Geological setting

Mesopotamian Basin is extended from north to south Iraq (Fig. 1a), which the Cretaceous oil habitat of the oil fields in southern Iraq is a result of many processes that started during the Triassic, when a new ocean began to form at the southern end of the Palaeo-Tethys Ocean [6]. The basin is an asymmetric fore deep, with a regional dip to the east-northeast [6]. In the basin, the base Upper Jurassic surface lies 2000–3500 m below sea level in the west, deepening to >6000 m below sea level in the east [6]. The western margin of the basin is interpreted to be bounded by significant NNW–SSE trending fault zones. The amount of displacement along these fault zones is poorly constrained and may be very limited [7].

The stratigraphic section in the southern Mesopotamian Basin is dominated by a thick Mesozoic succession and ranges in age from Jurassic to Cretaceous (Fig. 2). The Jurassic–Cretaceous depositional environment and hydrocarbon habitat have been studied by several researchers [4–6,8–11]. However, during Jurassic–Early Cretaceous time several sediments were deposited in the southern Iraq, which are include Sargelu, Najmah, Gotnia, and Sulaiy sediments (Fig. 2). The Middle Jurassic extends through northern and

southern of the basin. It is composed of thin bedded, bituminous limestone, dolomitic limestone and black shales [12]. The Sargelu Formation is considered as oil-source rock in the basin [6,7,13]. The Sargelu Formation is overlain conformably by the bituminous limestone of the Upper Jurassic Najmah Formation (Fig. 2). The Upper Jurassic Najmah Formation is extended into Kuwait and also is considered as oil-source rock [14,15]. The Najmah Formation is overlain conformably by Upper Jurassic Gotnia Formation, which is considered as the main seal rocks in south Iraq [16]. The Gotnia Formation is primarily composed of bedded evaporites with subordinate pseudo-oolitic limestone (Fig. 2). During latest Jurassic to Early Cretaceous time, the accumulation of carbonates in marine deposits of the Sulaiy Formation was accompanied in the basin (Fig. 2). The Sulaiy Formation contains bituminite limestones and black shales, which is considers as oil-source rock in the south Iraq [6]. The Sulaiy Formation has kerogen Type II-S and was deposited in marine anoxic conditions stratification [6]. This formation is overlain conformably by Cretaceous units (Fig. 2). The Cretaceous units comprise the Yamama, Ratawi, Zubair, Shuaiba, Nahr Umr, Maudud Ahmadi, Rumaila and Mishrif deposited during Early Cretaceous to Late Cretaceous time (Fig. 2). These sedimentary rocks are composed of mainly marine carbonates and subordinate

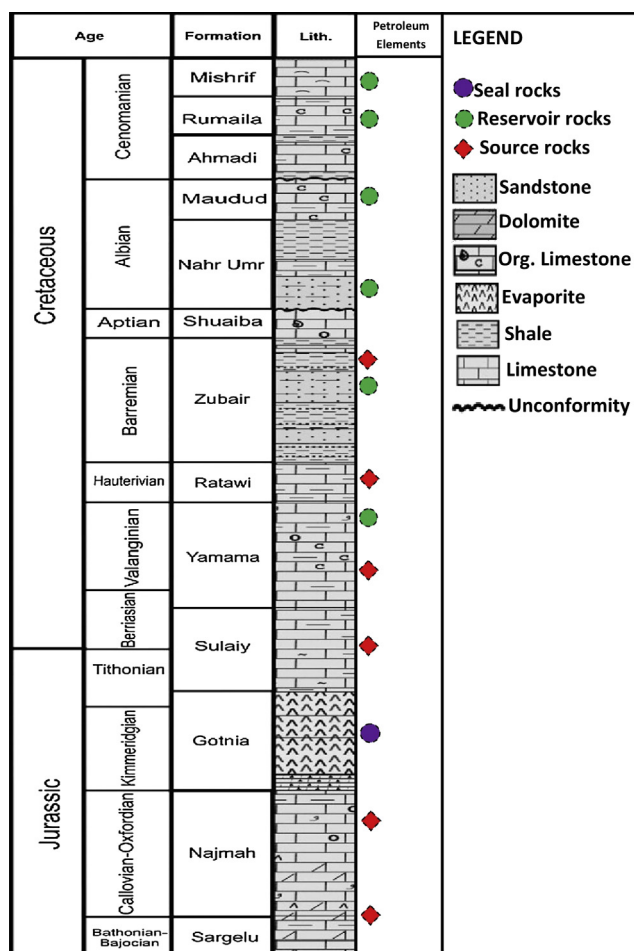


Fig. 2. Generalized stratigraphic column of Jurassic–Cretaceous sequences of southern Iraq showing petroleum elements (modified after Abeer et al., [11]).

clastics sediments (Fig. 2). The Cretaceous rocks in the basin are considered as gas and oil reservoir rocks [7] and comprise fractured and vuggy carbonates as well as clastic rocks (Fig. 2). How-

ever, the coastal plain sandstones of the Zubair Formation includes most of the oil reserves in several fields of southern Iraq, were deposited during Barremian time (Fig. 2). The Mishrif Formation is one of the main Cretaceous carbonate promising reservoirs in the Mesopotamian Basin, southern Iraq. The crude oil samples in this study were collected from this Mishrif carbonate reservoir rocks.

3. Samples and experimental methods

In this study, seven (7) crude oil samples representing Early Cretaceous Mishrif petroleum reservoir rock in the three oilfield (West Qurna, Zubair, and Nasriah), Southern Mesopotamian Basin (Fig. 1b; Table 1) were investigated using different analyses. These analyses include API gravity, measurement of sulfur content and trace elements (i.e. Ni, V), bulk carbon isotope, asphaltene precipitation, fractionation, gas chromatography–mass spectrometry (GC–MS). Most of the analyses were carried out at the GeoMark research Ins. Houston–Texas.

API gravity was performed on the crude oil samples, which is calculated from the density measured at 60°F. About 1–2 mL of whole oil is injected using a syringe into an Anton Par DMA 500 density meter. This process is triplicated for each oil in order to validate accuracy and reproducibility. The whole oil samples were also measured on a vario ISOTOPE select elemental analyzer for wt% sulfur via the process of dumas combustion.

The whole oil samples were treated to remove asphaltene by dissolved in an excess of *n*-pentane. The suspension of asphaltene was left for 5 min and then allowed to settle in a refrigerator for at least 1 h. The precipitated asphaltenes were then filtered. The C₁₅₊ deasphalted fractions were then separated into saturated hydrocarbon, aromatic hydrocarbon, and NSO (nitrogen-sulfur-oxygen compounds or resin) fractions using gravity-flow column chromatography employing a 100–200 mesh silica gel support activated at 400 °C prior to use. Hexane is used to elute the saturated hydrocarbons, methylene chloride to elute the aromatic hydrocarbons, and methylene chloride/methanol (50:50) to elute the NSO fraction. The saturated fraction was then analysed by a GC–MS instrument using an Agilent 7890A or 7890B GC interfaced to a 5975C or 5977A mass spectrometer. The GC compound sepa-

Table 1

Bulk property and chemical composition results of the crude oils from three oilfields (i.e., West Qurna, Zubair, and Nasriah) in the southern Mesopotamian Basin, South Iraq.

Oilfields	Wells	Samples ID	Reservoir/age	API (o)	S (%)	V ppm	Ni ppm	V/Ni	V/(V+Ni)	Fractions (wt%)				Isotope compositions (‰)	
										Sat.	Aro.	Res.	Asph.	Saturated	Aromatic
West Qurna oil field	WQ-41 well	IQ0171	Mishrif/Cenomanian to Turonian	23.2	4.84	102	27	3.78	0.79	22.9	54.0	12.8	10.4	–27.25	–27.49
	WQ-90 well	IQ0173	Mishrif/Cenomanian to Turonian	22.1	4.68	98	29	3.38	0.77	21.7	55.8	12.1	10.4	–27.33	–27.48
	WQ-201 well	IQ0176	Mishrif/Cenomanian to Turonian	21.0	4.22	63	15	4.20	0.81	19.8	54.7	9.3	16.2	–27.24	–27.31
	WQ-79 well	IQ0186	Mishrif/Cenomanian to Turonian	23.3	5.14	108	30	3.60	0.78	22.2	57.3	10.5	10.1	–27.44	–27.58
Zubair oil field	ZB-163	IQ0188	Mishrif/Cenomanian to Turonian	25.3	4.22	62	15	4.13	0.81	23.5	58.2	11.5	6.8	–27.16	–27.45
Nasriah oil field	NS-1	IQ0172	Mishrif/Cenomanian to Turonian	26.8	4.33	55	13	4.23	0.81	24.9	57.4	12.5	5.3	–27.24	–27.47
	NS-3	IQ0174	Mishrif/Cenomanian to Turonian	27.2	4.20	55	15	3.67	0.79	25.0	56.2	13.2	5.6	–27.23	–27.53

S – Sulfur.

V – Vanadium.

Ni – Nickel.

Sat. – Saturated hydrocarbons.

Aro. – Aromatic hydrocarbons.

Res. – Resin.

Asph. – Asphaltene.

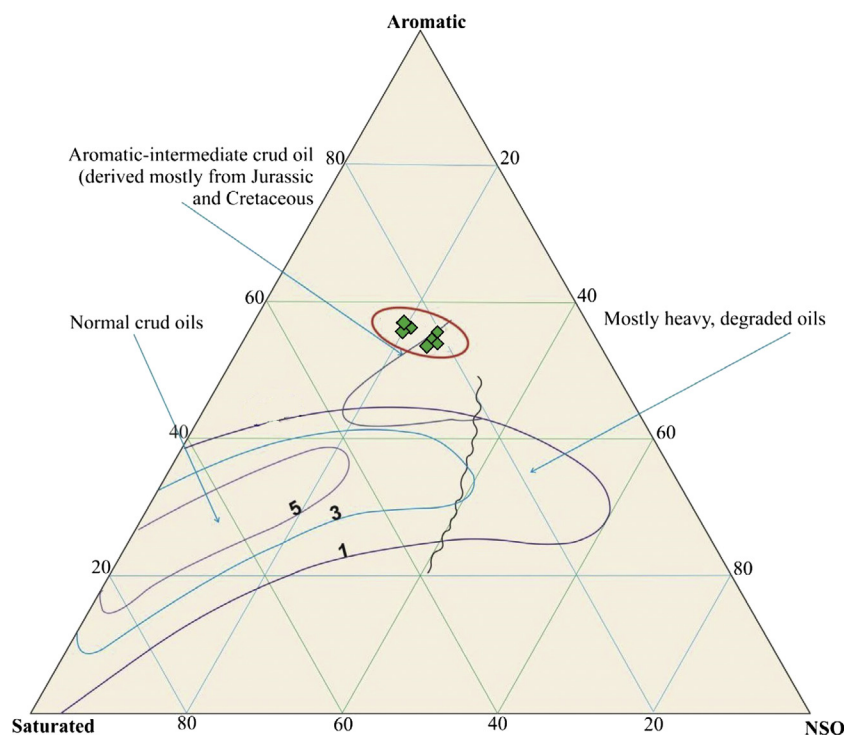


Fig. 3. Ternary diagram showing the gross composition: saturated hydrocarbons, aromatic hydrocarbons, and resins plus asphaltenes of analysed oils in selected oilfields of southern Iraq. (modified after Tissot and Welte, [23]).

ration was performed using a HP-5 column (length: 50 m, internal diameter: 0.2 mm, film thickness: 0.11 μm) and temperature programmed from 150 to 325 $^{\circ}\text{C}$ at a rate of 2 $^{\circ}\text{C}/\text{min}$, and then held for 30 min at 320 $^{\circ}\text{C}$. The selected ion monitoring (SIM) capabilities of the data acquisition system permitted specific ions to be monitored, such as terpanes (m/z 191), and steranes (m/z 217) of saturated hydrocarbons. Peak assignments for hydrocarbons in the GC–MS of saturated fractions in the m/z 191 and 217 mass fragmentograms are listed in Appendix 1.

Bulk stable carbon isotopic compositions ($^{13}\text{C}/^{12}\text{C}$) of C_{15+} saturate and aromatic hydrocarbon fractions are measured on an IsoPrime vario ISOTOPE select elemental analyzer and VisION isotope ratio mass spectrometer (IRMS). Results are reported as delta-notation relative to Pee Dee belemnite (PDB) by reference to the appropriate international standard.

4. Results

4.1. Bulk oil characteristics

The bulk characteristics of analysed oils are presented in Table 1, which include oil properties and compositions. These bulk characteristics include API gravity, sulfur content and maltene fractions of the oils (Table 1).

4.1.1. API gravity and sulfur content

The analysed oil samples from southern Mesopotamian Basin in this study have relatively low API gravity values in the range of 21.0–27.2 $^{\circ}$ (Table 1). API gravity can be used as a crude indicator of thermal maturity [17]. The lower API gravity values are also generally associated with either biodegraded oils or early-mature sulfur-rich oils [18]. In this study, the low API gravity values suggest early-mature sulfur-rich oils [18]. This finding is supported by high concentrations of sulfur (S) content in the analysed oil samples (Table 1), and indicates that low values of API gravity is associated with early-mature sulfur-rich oils [18].

The sulfur content also reflects a certain extent the type of organic input to the source rock and its environment conditions [19,20]. Carbonate source rocks deposited in a marine environment under reducing conditions generally have high sulfur contents, whereas source rocks deposited in siliciclastic environment usually have low sulfur contents [19]. In this study, the analysed oils have high sulfur contents ranging from 4.20 to 5.14 wt%, suggesting that the oils were derived from carbonate source rock deposited in a marine environment under sulphate-reducing conditions [19,21]. This is supported by the type of organic matter and environment conditions based on the biomarker environment parameters, which were discussed in the next subsections. Moreover, the high sulfur contents are also suggested that the analysed oils were generated from source rocks has a high-S kerogen (Type II-S). In addition, crude oils that contain considerable quantities of sulfur compounds (>0.5%) are called sour crude oils, whereas those with less sulfur (<0.42) are called sweet crude oils [22]. In this regard, the analysed oil samples are classified as sour crude oils, with high sulfur content for the analysed oil samples (Table 1).

4.1.2. Oil fractionation

The whole crude oils were fractionated into saturated and aromatic (hydrocarbons) and resin and asphaltene (NSO) compounds. The relative proportions of saturated, aromatic and NSO compounds are presented in Table 1. The hydrocarbons (i.e., saturate and aromatic) represent major fractions of the analysed oil samples, and consequently they have a relatively low NSO component (Table 1). These fractions are very important in oil classification [23]. However, the relative percentages of oil fractions (i.e., saturate, aromatic and NSO) are also plotted in a ternary diagram of Tissot and Welte [23]. The Mishrif oils have high aromatic hydrocarbons and are classified as aromatic intermediate oils (Fig. 3). These types of oil were derived mostly from Jurassic and Cretaceous source rocks [23].

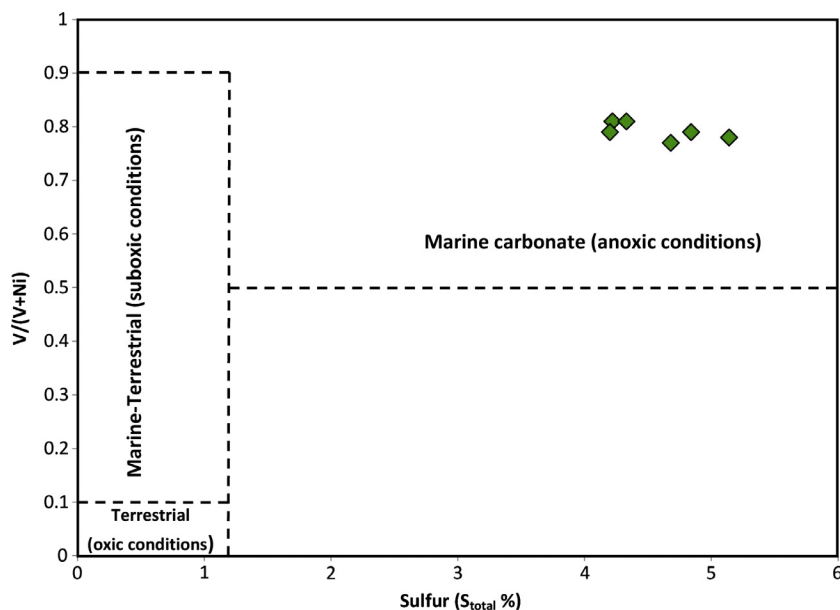


Fig. 4. Trace element ratios of $V/(V + Ni)$ versus sulfur content (wt%) of the analysed oil samples.

4.2. Nickel and vanadium contents

Crude oils contain metals; particularly nickel (Ni) and vanadium (V), in variable amounts. Ni and V metals exist in petroleum largely as porphyrin complexes, and enter into the porphyrin structure by chelation during early diagenesis. The Ni and V metals are usually associated with the heavy, polar NSO fraction of crude oils and, as such, should increase in concentration with evaporation, biodegradation and other environmental processes acting preferentially on the light ends of the oil [24]. However, the V and Ni concentrations and their V/N ratios can be used to classify and correlate crude oils [25]. Although the V and Ni concentrations in oils are quite dependent upon the degree of oil alteration such as biodegradation and maturity, the concentrations of the V and Ni metals in oils can also be provides insight into the depositional environment condi-

tions of their potential source rocks [26,27]. In general, oils generated from marine carbonate or siliciclastic source rocks show moderate to high sulfur and high concentrations of Ni and V metals [26]. This is consistent with the high values of Ni and V metals sulfur contents of the analysed oil samples (Table 1). The relatively high $V/(V + Ni)$ ratios and sulfur contents further suggest that the analysed oils were derived from marine carbonate source rock that deposited under reducing (anoxic) conditions (Fig. 4).

4.3. Stable carbon isotope composition

The stable carbon isotopic composition of oils is an important tool with which to differentiate depositional environments of their source rocks and to determine the genetic relationship between oils and their potential source rocks [28–31]. Sofer [28] suggested

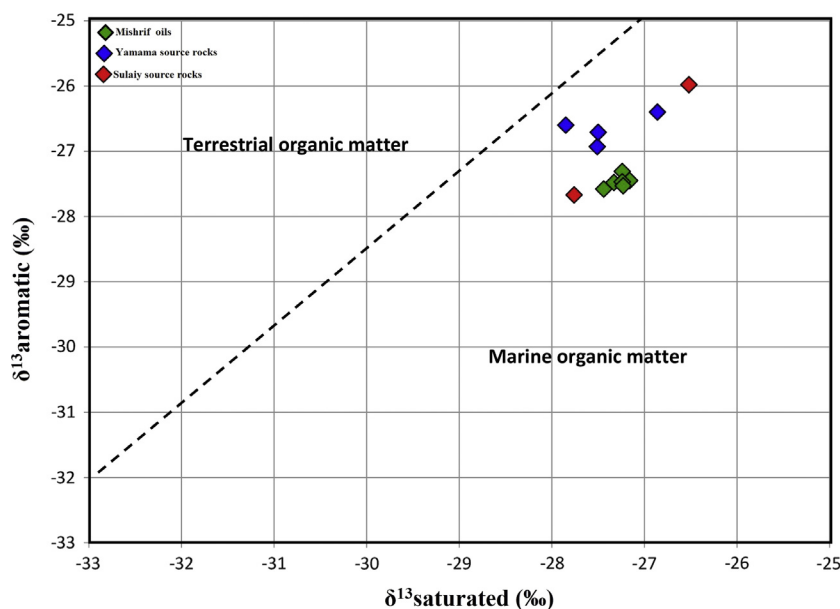


Fig. 5. Plot of the $\delta^{13}C$ values of aromatic fractions versus of the $\delta^{13}C$ values of saturated fractions for analysed oils samples and the Late Jurassic–Early Cretaceous Sulaiy and Yamama source rocks in the basin. The line represents the best fit separation for waxy and non-waxy oils and is described by the equation $\delta^{13}C \text{ Aromatic} = 1.14 \delta^{13}C \text{ saturated} + 5.46$ (after Sofer, 1984).

diagram of bulk values of the $\delta^{13}\text{C}$ saturated fractions versus those of their aromatic fractions and used to classify the environments of oils and source rock as marine or non-marine (terigenous). The analysed oil samples have $\delta^{13}\text{C}$ values of their saturated and aromatic hydrocarbon fractions range from -27.16‰ to -27.44‰ and -27.31‰ to -27.58‰ , respectively (Table 1), which are plotted on a bulk fraction isotope plot defined by Sofer [28]. From the plot of bulk $\delta^{13}\text{C}$ saturated and aromatic fractions, the Mishrif oils are derived from marine source rocks (i.e., Sulaiy and Yamama) (Fig. 5).

4.4. Biomarker distributions

In this study, the biomarker distributions were examined by the *n*-alkane, isoprenoid, hopane and sterane components. Individual saturated biomarker components were identified by comparison of the retention times and mass spectra of the monitored ions for

terpanes and hopanes (*m/z* 191) and steranes (*m/z* 217) whereby their mass fragmentograms were compared with previously published work [22,32]. The biomarker ratios were calculated by measuring peak heights in the fragmentograms.

Normal alkanes and isoprenoids are represented by a full suite of saturated hydrocarbons between C_4 – C_{35} *n*-alkanes and isoprenoids, and show unimodal *n*-alkane distributions with dominance of short-chain *n*-alkanes (C_4 – C_{15}) relative to long chain *n*-alkanes (C_{20} – C_{35}) with *n*-alkane maximum in the range of C_6 – C_9 (Fig. 6). These *n*-alkane distributions giving low values of carbon preference index (CPI) in the range of 0.83–0.92 (Table 2).

Gas chromatograms of the saturated hydrocarbon fractions also show acyclic isoprenoids (i.e. pristane and phytane). Phytane (Ph; C_{20}) is almost always higher than Pristane (Pr; C_{19}) (Fig. 6), resulting in a relatively narrow range of Pr/Ph ratio from 0.75 to 0.84 (Table 2). Furthermore, the amounts of isoprenoids compared to *n*-alkanes based on pristane/*n*- C_{17} and phytane/*n*- C_{18} ratios have

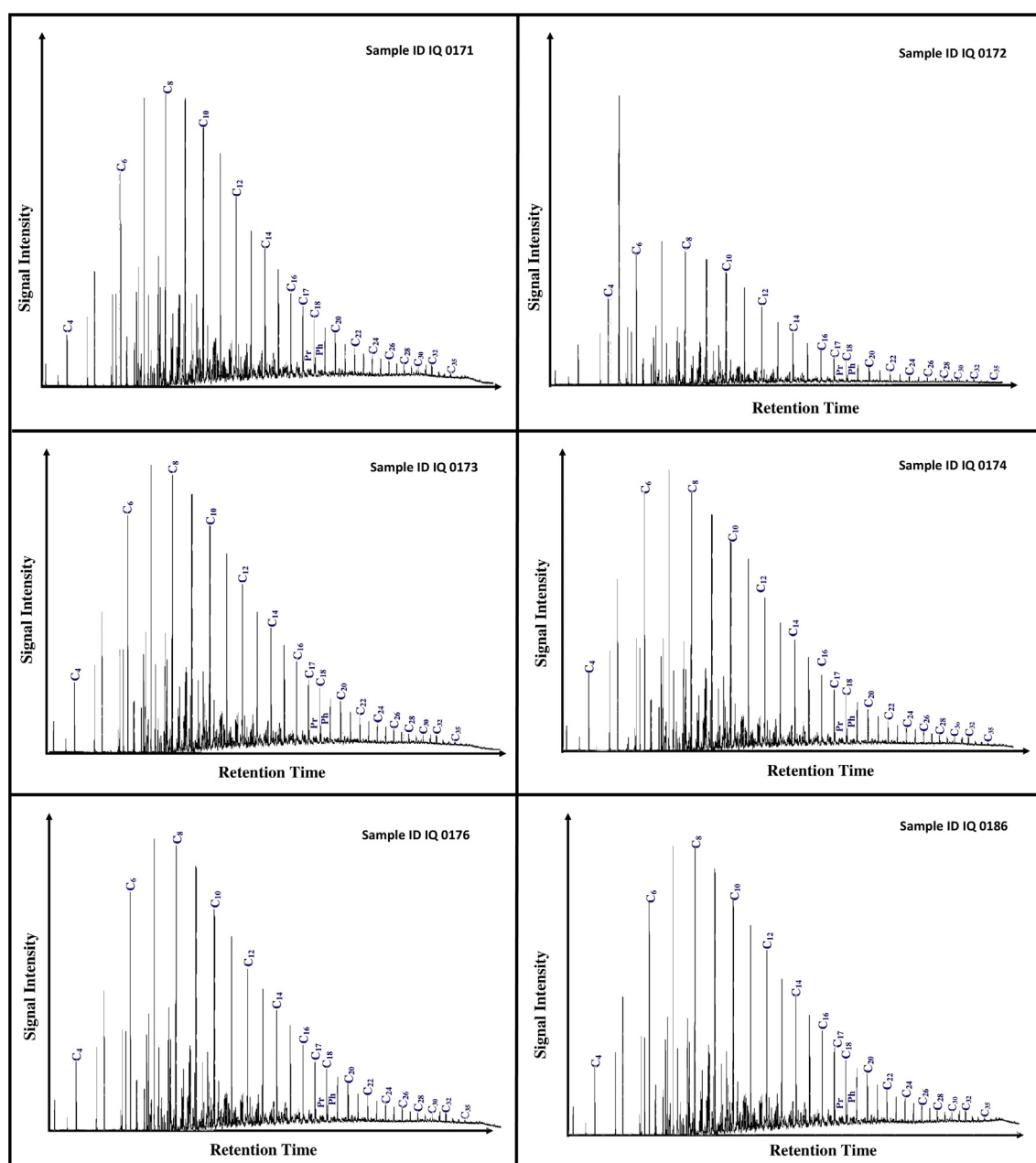


Fig. 6. Gas chromatograms of saturated hydrocarbon fraction of six representative analysed oil samples.

Table 2

Selected biomarker parameters of the crude oil samples from southern Mesopotamian Basin, South Iraq, illustrating source organic matter, depositional environment conditions and thermal maturity.

Samples ID	n-alkane and isoprenoids				Triterpanes and terpanes (m/z191)								Steranes (m/z217)						
	Pr/Ph	Pr/C ₁₇	Ph/C ₁₈	CPI	C ₃₂ 22S/ (22S + 22R)	MC ₃₀ / C ₃₀	C ₂₉ / C ₃₀	Ts/ Tm	G/ C ₃₀	C ₃₅ Ho/ C ₃₄ Ho	HOI	HCR ₃₁ / HC ₃₀	C ₂₉ 20S/ 20S + 20R	C ₂₉ ββ/ (ββ + αα)	Diastereane/ sterane	C ₂₉ /C ₂₇ Regular steranes	Regular steranes (%)		
																C ₂₇	C ₂₈	C ₂₉	
IQ0171	0.84	0.23	0.34	0.92	0.53	0.09	1.72	0.17	0.25	1.05	0.10	0.34	0.37	0.44	0.12	0.90	45.56	13.28	41.16
IQ0173	0.80	0.22	0.32	0.82	0.52	0.09	1.64	0.17	0.23	1.10	0.09	0.34	0.40	0.46	0.12	0.81	46.99	14.76	38.25
IQ0176	0.82	0.23	0.32	0.90	0.53	0.08	1.69	0.17	0.24	1.06	0.11	0.33	0.40	0.44	0.12	0.80	48.04	13.47	38.49
IQ0186	0.75	0.21	0.33	0.87	0.51	0.08	1.66	0.17	0.23	1.06	0.12	0.33	0.38	0.44	0.13	0.88	45.54	14.48	39.98
IQ0188	0.79	0.19	0.31	0.83	0.52	0.09	1.73	0.18	0.26	1.04	0.10	0.33	0.37	0.44	0.12	0.87	46.26	13.57	40.18
IQ0172	0.82	0.23	0.32	0.83	0.52	0.08	1.67	0.18	0.23	1.07	0.11	0.33	0.38	0.45	0.12	0.82	47.07	14.39	38.54
IQ0174	0.79	0.22	0.33	0.84	0.53	0.08	1.60	0.18	0.24	1.11	0.10	0.32	0.38	0.44	0.13	0.86	46.59	13.29	40.13

Pr – Pristane; Ts – (C₂₇ 18α(H)-22,29,30-trisnorhopane); CPI – Carbon preference index (1): $\{2(C_{23} + C_{25} + C_{27} + C_{29}) / (C_{22} + 2[C_{24} + C_{26} + C_{28}] + C_{30})\}$.

Ph – Phytane; Tm – (C₂₇ 17α(H)-22,29,30-trisnorhopane); HCR₃₁/HC₃₀: C₃₁ regular homohopane/C₃₀ hopane.

HOI: homohopane index = C₃₅ (R+S)/total homohopanes C₃₁ – C₃₅ (R+S); C₃₀M/C₃₀H = C₃₀ moretane/C₃₀ hopane; C₂₉/C₃₀: C₂₉ norhopane/C₃₀ hopane.

C₃₅Ho/C₃₄Ho = C₃₅ homohopane/C₃₄ homohopanes G/HC₃₀ = Gammacerane/C₃₀ hopane.

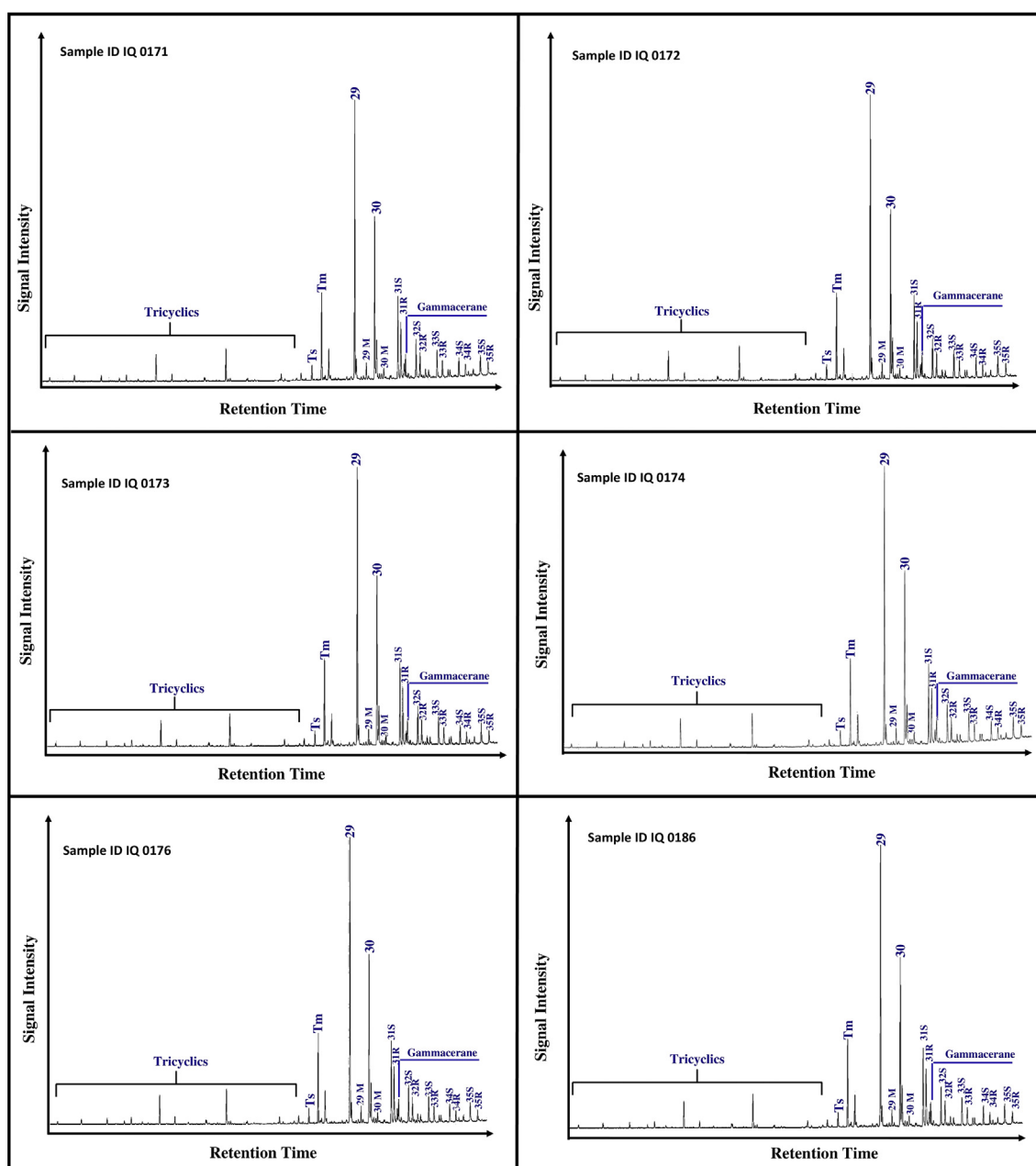


Fig. 7. Terpanes distribution in the *m/z* 191 mass fragmentograms in the saturated fraction of six representative oil samples.

also been calculated, thus giving low pristane/n-C₁₇ and phytane/n-C₁₈ ratios in the range of 0.19–0.23 and 0.31–0.34, respectively (Table 2).

On the other hand, the terpane and sterane are other important biomarkers that are commonly detected in *m/z* 191 and *m/z* 217 ion fragmentograms, respectively. The tricyclic terpanes as well as the hopanes were detected in the *m/z* 191 mass fragmentograms in all the analysed oil samples as shown in Fig. 7. The *m/z* 191 mass fragmentogram of the saturated hydrocarbon fractions shows high proportions of hopanes relative to tricyclic terpanes (Fig. 7). The hopane biomarkers are dominated by the presence of C₃₀-hopane and C₂₉-norhopane, with significant presence of 18 α (H)-trisorhopane (Ts), and a considerable quantity of homohopanes (C₃₁–C₃₅) (Fig. 7). The C₂₉-norhopane is higher in all of the analysed oil samples (Fig. 8), with C₂₉/C₃₀ ratios more than 1 (Table 2). The predominance of C₂₉-norhopane is consistent with carbonate source rock [33].

The homohopane distributions are dominated by the C₃₁ homohopane and generally decreasing toward the C₃₅ homohopane (Fig. 7). The ratios of the homohopane distribution i.e., C₃₁-22R-hopane/C₃₀-hopane and homohopane index [C₃₅/(C₃₁ + C₃₅)] ratios have been calculated (Table 2) and used to define the depositional environment conditions [22]. In this study, the analysed oil samples have C₃₁-22R-hopane/C₃₀-hopane and homohopane index in the range of 0.32–0.34 and 0.09–0.12, respectively (Table 2). In addition, gammacerane has been recorded in significant amounts in the analysed oil samples (Fig. 7), whereby variable gammacerane index (gammacerane/C₃₀ hopane) in the range of 0.23–0.26 (Table 2) was obtained.

The sterane and diasterane biomarkers have also been recognized in the analysed oil samples (Fig. 8). The *m/z* 217 mass fragmentograms of all the analysed oil samples are dominated by steranes over diasteranes, with high concentrations of C₂₇ regular steranes (Fig. 8). Relative abundances of C₂₇, C₂₈ and C₂₉ regular steranes

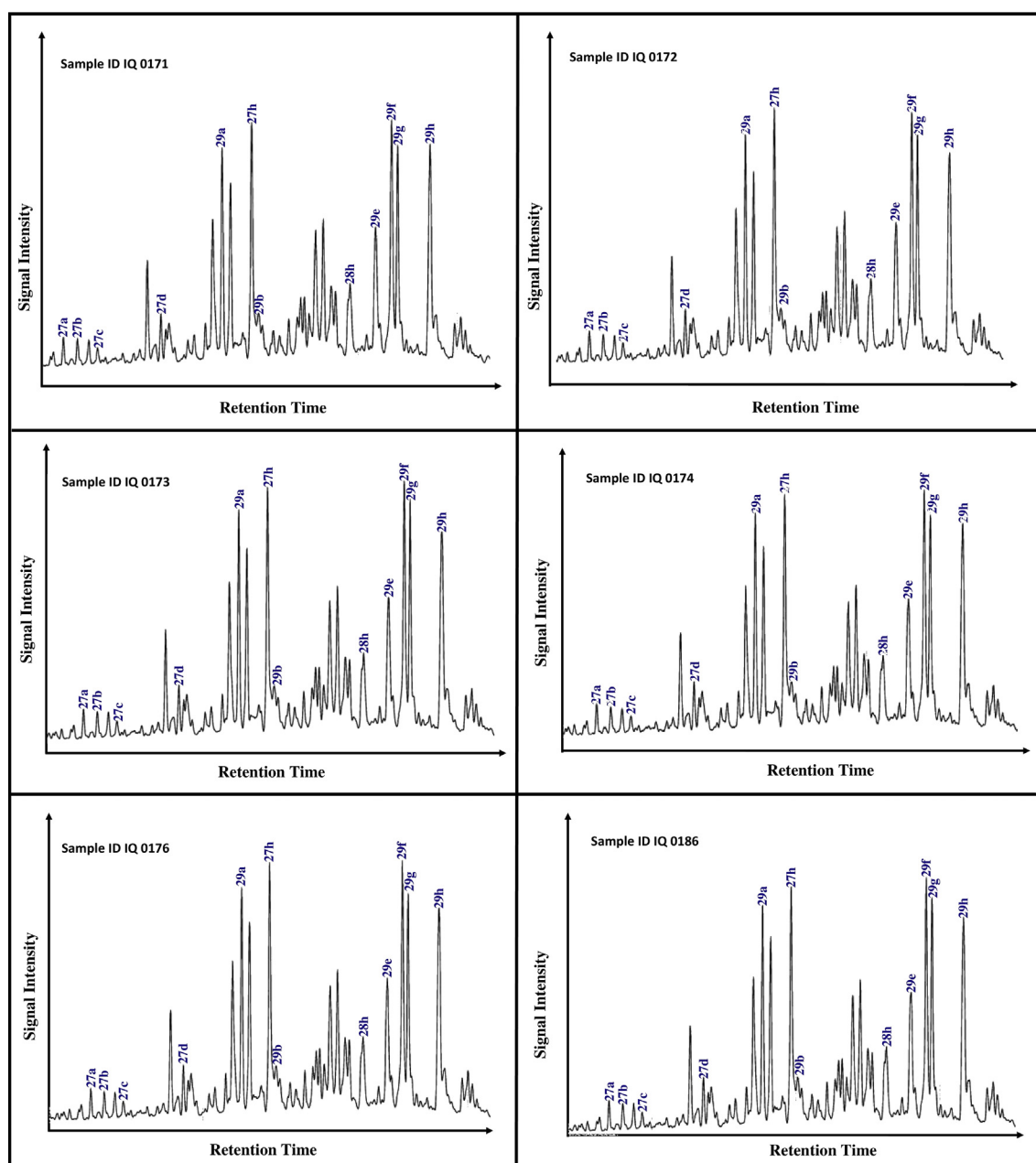


Fig. 8. Steranes and diasteranes distribution in the *m/z* 217 mass fragmentograms in the saturated fraction of six representative oil samples.

were also calculated and the results show that the analysed oil shales have a high proportion of C_{27} (45.54–48.04%) compared to C_{29} (38.25–41.16%) and C_{28} (13.28–14.76%) regular steranes (Table 2). The ratios of C_{29}/C_{27} regular sterane, diasterane/sterane and maturity ratios i.e., C_{29} sterane $20S/(20S + 20R)$ and $\beta\beta/(\beta\beta + \alpha\alpha)$ have also been calculated and the results are given in Table 2.

5. Discussion

5.1. Biodegradation of crude oils

The bacteria involved in the biodegradation process in an oil reservoir and the process dramatically affects the fluid properties

of the hydrocarbons [34] due to temperature limit [35]. However, the basic signs of biodegradation are well established in this study and indicate that there is no biodegradation observed in the analysed oil samples. This is concluded from the shape of gas chromatograms of the oil samples (Fig. 6), where the analysed oils contain a complete suite of *n*-alkanes in the low-molecular weight region and acyclic isoprenoids [36]. The amounts of isoprenoid compared to *n*-alkanes, with low pristane/ n - C_{17} and phytane/ n - C_{18} ratios further suggest the oil samples were not biodegraded (Fig. 9). This is consistent with low concentrations of NSO components (i.e., resin and asphaltene) compared to hydrocarbon fractions (saturated and aromatic) (Table 1). Thus the high NSO contents are likely a result of a biodegradation process among the oil samples [22].

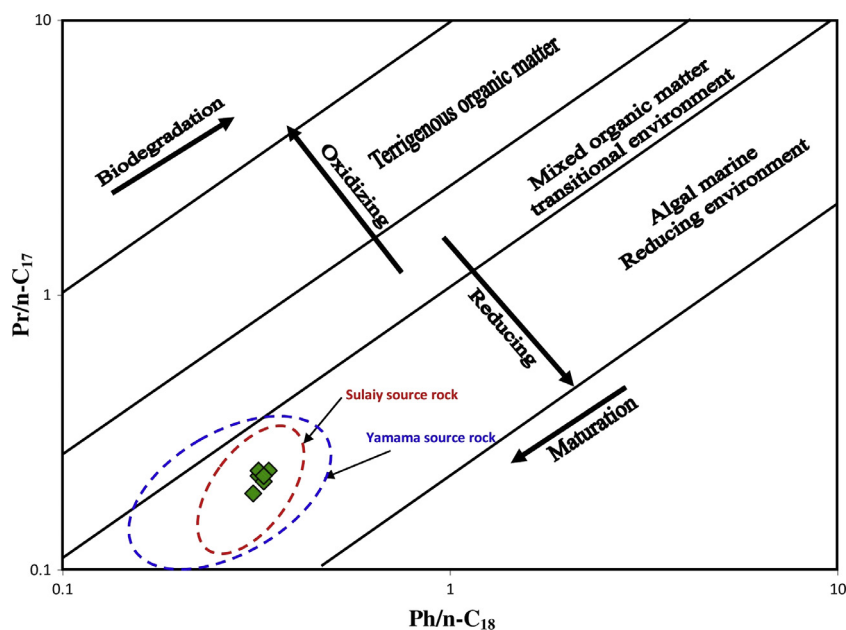


Fig. 9. $Pr/n-C_{17}$ ratio versus $Ph/n-C_{18}$ ratios of the analysed oil samples and zones of the Late Jurassic–Early Cretaceous Sulaiy and Yamama source rocks in the basin (after Abeed at al., [6]).

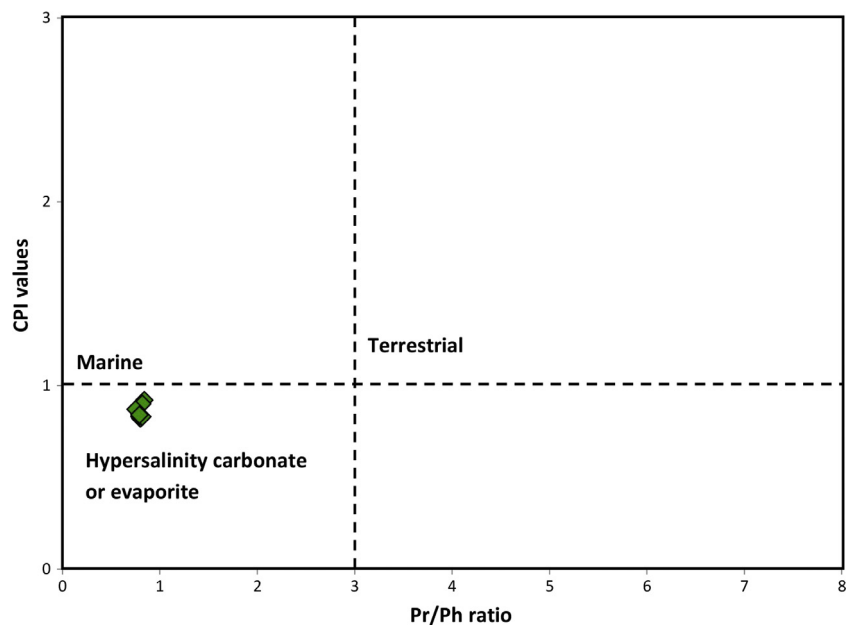


Fig. 10. Cross plot of CPI and pristane/phytane ratio of the analysed oil samples, showing marine hypersaline carbonate source rock (modified after Hubred, 2006).

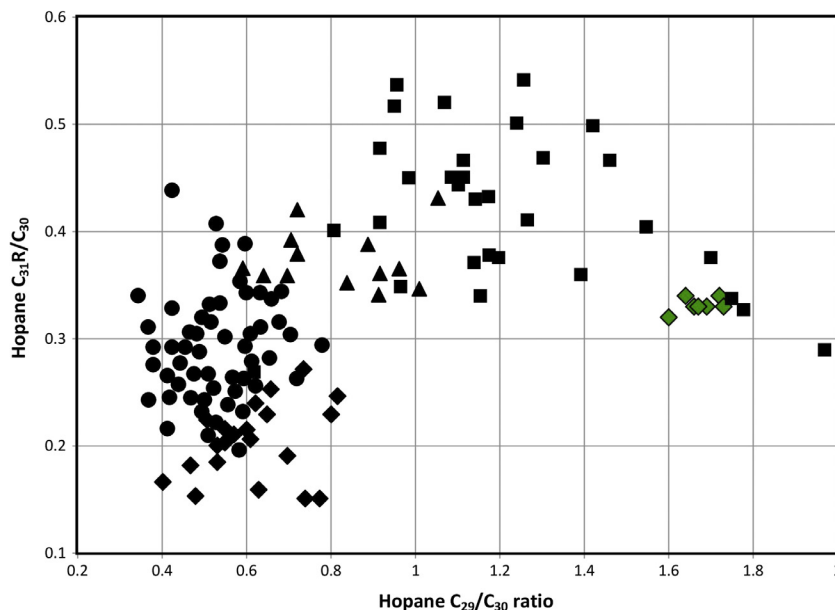


Fig. 11. Average hopane ratios of analysed oils from southern Iraq suggesting a carbonate source rock (SR). Other data points represent average oil values from 150 global petroleum systems from marine carbonate, distal marine shale, marine marl, and lacustrine shale source rocks.

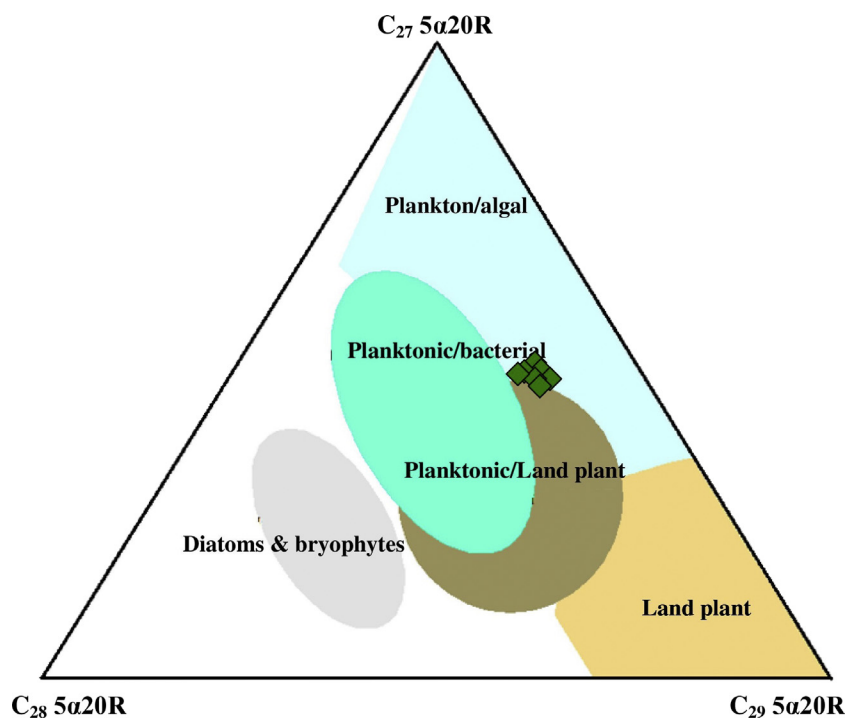


Fig. 12. Ternary diagram of regular steranes (C_{27} – C_{29}) indicating the relationship between sterane compositions in relation to organic matter input and depositional environments (modified after Huang and Meinschein, 1979).

5.2. Depositional environment conditions and organic matter input

In this study, the depositional paleoenvironment and conditions of organic matter input of the source rock that expelled the studied oil were primarily based on biomarker and non biomarker results as presented in the previous subsections. The n -alkane distributions of the saturated hydrocarbon for the analysed oil samples are characterized by a predominance of low to moderate molecular weight compounds (Fig. 6) and suggest a high contribution of mar-

ine organic matter input (i.e., algal and cyanobacterial) [37–40]. The predominantly marine origin of organic matter confirms from bulk values of the $\delta^{13}C$ saturated and aromatic fractions (Fig. 5). These characteristics, along with low value of Pr/Ph, pristane/ n - C_{17} and phytane/ n - C_{18} ratios are typical of source rock with high contributions of marine algal organic matter (Fig. 9). Moreover, the acyclic isoprenoids i.e., pristane (Pr) and phytane (Ph) are usually used to define the depositional conditions (anoxic versus oxic) [22,41–44]. The low Pr/Ph ratios (<1) of the analysed oil also

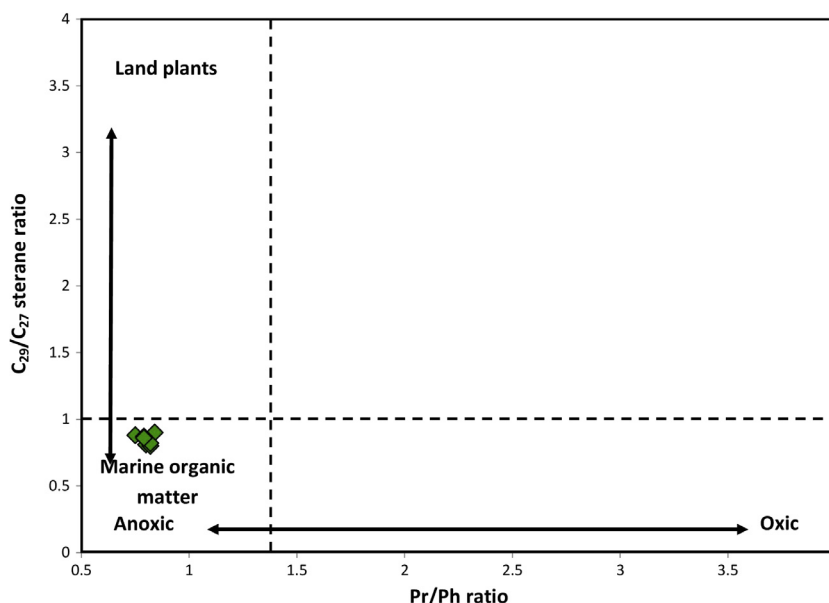


Fig. 13. Cross-plots for pristane/phytane versus C_{29}/C_{27} regular steranes ratio, which provides an inference for a source rock deposit environment and lithology (modified after Peters et al. 2005).

indicate that the marine organic matter was preserved under reducing (anoxic) conditions [42,43]. The relatively low carbon preference index values ($CPI < 1$) that obtained in this study further suggest that the analysed oil samples were generated from marine carbonate source rock (Fig. 10).

Furthermore, terpane biomarker ratios (Table 2) also suggest that the analysed oil samples were derived from marine carbonate source rock that deposited under anoxic and hypersalinity conditions. A high concentrations of C_{29} -norhopane compared to C_{30} -hopane is consistent with carbonate source rock [33]. This is confirmed by the high values of C_{31} -22R-hopane/ C_{30} -hopane ratio (Fig. 11), since the C_{31} -22R-hopane/ C_{30} -hopane ratios more than 0.30 indicate marine carbonate source rocks [22]. However, the homohopanes distributions of C_{31} - C_{35} in term of homohopanes index can be used to evaluate redox conditions during deposition of the source rock [22]. The analysed oils have relatively high homohopane indices (Table 2), suggesting anoxic conditions [22,44]. This is consistent with the relatively high homohopane C_{35} concentrations compared to C_{34} homohopane (Fig. 7), with high C_{35}/C_{34} ratios (Table 2). In addition, the presence of gammacerane biomarker in the oil samples (Fig. 7) is a strong indicator of sulphate-reducing conditions during deposition of source rock [20,45,46].

The depositional paleoenvironment and origin of organic matter can also be indicated from the distribution of C_{27} to C_{29} regular steranes in the m/z 217 mass fragmentograms of the saturated hydrocarbon fraction of all the oil samples (Fig. 8). As shown in the m/z 217 mass fragmentograms, the saturated hydrocarbon fraction is characterized by high abundances of C_{27} regular steranes compared to the C_{28} and C_{29} regular steranes (Fig. 8; Table 2). This can also be indicative of higher marine planktonic-bacterial organic matter [22,44] as indicated by the regular sterane ternary diagram (Fig. 12; [47]) and corroborated by low C_{29}/C_{27} regular sterane ratios (Fig. 13). The non biomarker parameters i.e., S, V and Ni contents have also been used as a broad proxy used to infer source of organic matter input (e.g. terrestrial versus marine) and depositional conditions (e.g. oxic versus anoxic) (see Subsections 4.1.1. and 4.2). However, the relationship between both of them

confirms a marine carbonate source rock deposited under anoxic conditions (Fig. 4).

5.3. Maturity of crude oils

The maturity of the analysed oil samples from oilfield in the southern Mesopotamian Basin was primary evaluated using specific biomarker ratios and coupled with non-biomarker parameters as presented in the Tables 1 and 2.

From m/z 191 and m/z 217 mass chromatograms of the saturated hydrocarbon fraction, the specific maturity biomarker ratios i.e., C_{32} hopanes $22S/(22S + 22R)$, Ts/Tm , C_{29} sterane $20S/(20S + 20R)$ and $\beta\beta/(\beta\beta + \alpha\alpha)$ ratios (Table 2) were used as maturity indicators [48–50]. A widely used biomarker maturity ratio is the C_{32} $22S/(22S + 22R)$ hopane ratio [22]. The values in the range 0.50–0.54 have barely entered the zone of oil generation, while ratios in the range 0.57–0.62 indicate that the main phase of oil generation has been reached or surpassed [44]. Most of the analysed oil samples have C_{32} hopanes are between 0.51 and 0.53 (Table 2), suggesting that they have reached oil window and the oils were generated from early mature source rocks [49]. This level of maturity of oils is also estimated from the $20S/(20S + 20R)$ and $\beta\beta/(\beta\beta + \alpha\alpha)$ C_{29} sterane ratios as these ratios increase with increasing maturity [49]. The analysed oil samples have low values of C_{29} sterane $20S/(20S + 20R)$ and $\beta\beta/(\beta\beta + \alpha\alpha)$ maturity ratios in the range of 0.37–0.40, 0.44–0.46 (Table 2), suggesting mostly either at or close to thermal equilibrium, consistent with their generation from early-mature source rocks [48,49] as shown in Fig. 14.

The ratio of the Ts and Tm biomarkers in the term $Ts/(Ts + Tm)$ ratio is also used as maturity indicator [22,44,51,52], which the Ts is more stable to thermal maturation than Tm . However, the $Ts/(Ts + Tm)$ ratios increase with increasing maturity [22,51,52]. The low values of the Ts/Tm ratio (0.17–0.18) reflects the same interpretation (early mature) as do the relationship between isoprenoids $Pr/n-C_{17}$ and $Ph/n-C_{18}$ ratios (Fig. 9).

Non-biomarker parameters i.e., API gravity, sulfur and metal contents (i.e., Ni, V) have also been used to evaluate the level of thermal maturity of the oils [53]. The concentration of Ni and V metals and sulfur content varied strongly with the maturity of oils

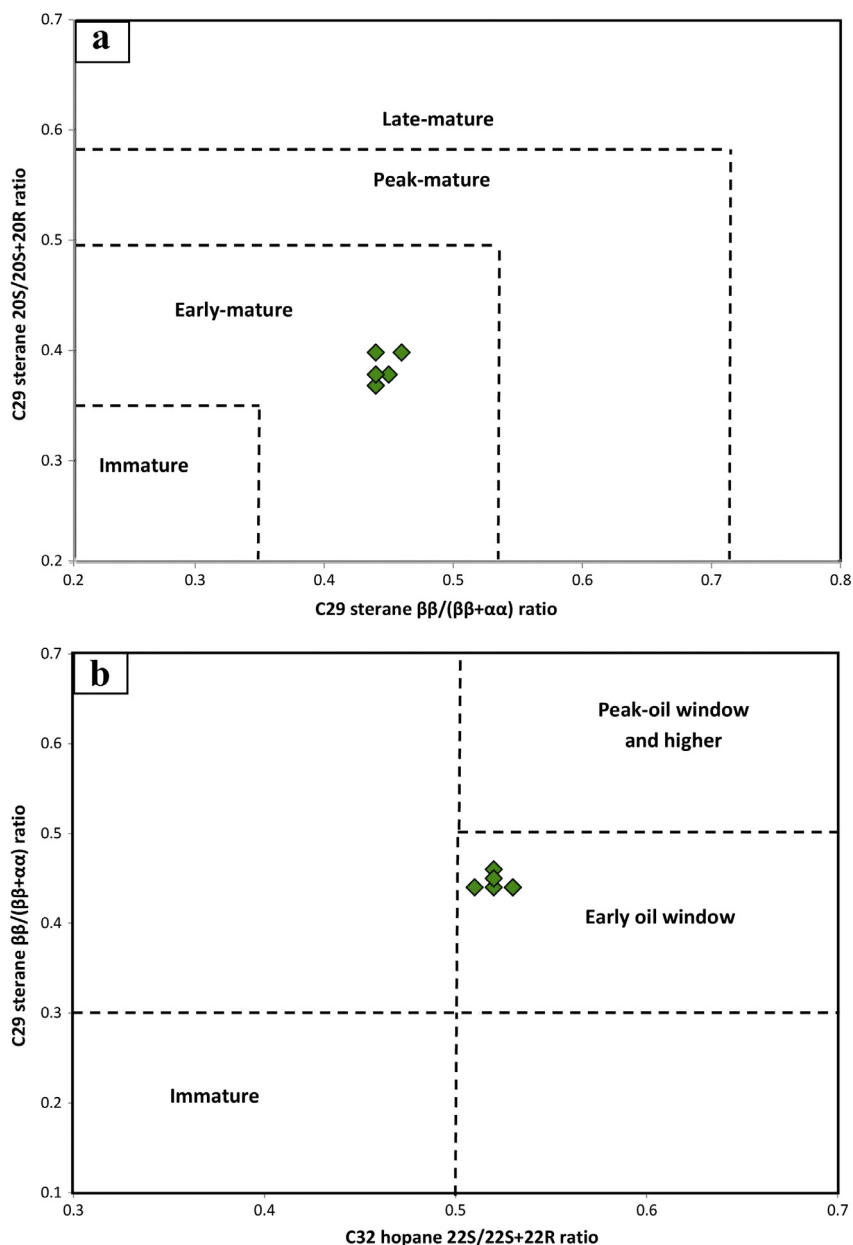


Fig. 14. A range of thermal maturity based on biomarker maturity parameters (a) C₂₉ sterane 20S/(20S + 20R) versus $\beta/(\beta + \alpha)$ as modified after Peters et al. (2005) and (b) C₃₂ hopane 22S/(22S + 22R) versus C₂₉ sterane $\beta/(\beta + \alpha)$ as modified after Peters and Moldowan (1993).

[27,53] (Barwise, 1990; El-Gayar et al., 2002). The levels of Ni and V metal and sulfur in crude oil decrease with increasing maturity, whereas the API gravity values increase [26,53]. The low values of the API and high S and metal (i.e., Ni, V) contents as shown in the Table 1 further suggest that the analysed oil samples were generated from early-mature source rock. This is consistent with previous biomarker observations.

5.4. Oil-source rock correlation

The results of the non-biomarker and biomarker parameters as presented in the previous subsections indicate that the analysed crude oils are aromatic intermediate sour crude oils and were derived from a marine carbonate source rock bearing Type II-S kerogen that was deposited under sulphate-reducing conditions.

The genetic link between the analysed oils and their potential source rocks were investigated using previous published works on the potential source rocks in the southern Mesopotamian Basin [6]. The most important potential source rocks in the southern Mesopotamian Basin are Late Jurassic to Early Cretaceous Sulaiy and Yamama source rocks [6]. These source rocks were deposited in a carbonate-rich, anoxic marine environment [6]. They also have high sulfur contents [6] suggest the presence of kerogen Type II-S, and thus have to be generated early-mature sulfur-rich oils. The source rock characteristics of the Sulaiy and Yamama formations are similar to those of the analysed oils in this study. The similarity has been achieved from biomarker and carbon isotope results of both source rocks and oils (Figs. 5 and 9). Therefore, the Late Jurassic to Early Cretaceous Sulaiy and Yamama source rocks are likely possible source rocks for the analysed oils in this study.

6. Conclusions

Biomarker and non-biomarker results were used to investigate the geochemical characteristics of the numerous crude oils in the southern Mesopotamian Basin, South Iraq. The conclusions from this study can be summarized as followed:

1. The analysed oils are characterized by relatively low API gravity, high sulfur and aromatic hydrocarbon fractions, indicating that the oils are aromatic intermediate sour oils and were generated from a source rock bearing high-S kerogen (Type II-S).
2. The oils were derived predominantly from a marine carbonate source rock received high abundance of plankton/algal and microorganism organic matter. This is achieved from their biomarkers of *n*-alkane, regular isoprenoid, terpane and sterane and bulk carbon isotopic compositions of their saturated and aromatic fractions.
3. Sulphate-reducing conditions during deposition of the source rocks have been evidenced from narrow Pr/Ph ratios and high elemental V/Ni ratios, high C₃₅ homohopane index and C₃₅/C₃₄ hopane ratios and the presence of gammacerane biomarker.
4. The biomarker and bulk carbon isotopic results of the oils in this study are similar to those of the Late Jurassic-Early Cretaceous source rocks in the basin (Abeed et al., 2011).
5. Biomarker maturity ratios and non-biomarker data such as low API gravity, high sulfur and trace metal (Ni, V) contents also indicate that the oils were generated from early-mature source rocks.

Acknowledgements

The authors are sincerely grateful to the South Oil Company in Iraq for supplying the oil samples to complete this study. Great acknowledgments are also given to John Zumberge for carrying out the geochemical analyses of the oil samples in GeoMark research Ins. Houston –Texas.

Appendix A

Peak assignments for alkane hydrocarbons in the gas chromatograms of saturated fractions in the *m/z* 191 (I) and 217 (II) mass fragmentograms.

(I) Peak no.	Compound abbreviation	
Ts	18 α (H),22,29,30-trisnorhopane	Ts
Tm	17 α (H),22,29,30-trisnorhopane	Tm
29	17 α ,21 β (H)-nor-hopane	C ₂₉ hop
30	17 α ,21 β (H)-hopane	Hopane
29M	17 β (H),21 α (H)-hopane (moretane)	C ₂₉ Mor
30M	17 β ,21 α (H)-Moretane	C ₃₀ Mor
31S	17 α ,21 β (H)-homohopane (22S)	C ₃₁ (22S)
31R	17 α ,21 β (H)-homohopane (22R)	C ₃₁ (22R)
32S	17 α ,21 β (H)-homohopane (22S)	C ₃₂ (22S)
32R	17 α ,21 β (H)-homohopane (22R)	C ₃₂ (22R)
33S	17 α ,21 β (H)-homohopane (22S)	C ₃₃ (22S)
33R	17 α ,21 β (H)-homohopane (22R)	C ₃₃ (22R)
34S	17 α ,21 β (H)-homohopane (22S)	C ₃₄ (22S)
34R	17 α ,21 β (H)-homohopane (22R)	C ₃₄ (22R)
35S	17 α ,21 β (H)-homohopane (22S)	C ₃₅ (22S)
35R	17 α ,21 β (H)-homohopane (22R)	C ₃₅ (22R)
(II) Peak no.		
a	13 β ,17 α (H)-diasteranes 20S	Diasteranes
b	13 β ,17 α (H)-diasteranes 20R	Diasteranes
c	13 α ,17 β (H)-diasteranes 20S	Diasteranes
d	13 α ,17 β (H)-diasteranes 20R	Diasteranes
e	5 α ,14 α (H), 17 α (H)-steranes 20S	$\alpha\alpha\alpha$ 20S
f	5 α ,14 β (H), 17 β (H)-steranes 20R	$\alpha\beta\beta$ 20R
g	5 α ,14 β (H), 17 β (H)-steranes 20S	$\alpha\beta\beta$ 20S
h	5 α ,14 α (H), 17 α (H)-steranes 20R	$\alpha\alpha\alpha$ 20R

References

- [1] J.A. Al-Sakini, Summary of petroleum geology of Iraq and the Middle East, Northern Oil Company Press, Kirkuk, 1992, p. 179 (in Arabic).
- [2] F.N. Sadooni, Stratigraphic sequence, microfacies, and petroleum prospects of the Yamama Formation, Lower Cretaceous, Southern Iraq, Am. Assoc. Pet. Geol. Bull. 77 (1993) 1971–1988.
- [3] F.N. Sadooni, A.M. Aqrabi, Cretaceous Sequence Stratigraphy and Petroleum Potential of the Mesopotamian Basin, Iraq. Special Publication 69, Society for Sedimentary Geology, 2000, ISBN 1-56576-075-1, pp. 315–334.
- [4] J.K. Pitman, D. Steinhauer, M.D. Lewan, Petroleum generation and migration in the Mesopotamian Basin and Zagros Fold Belt of Iraq: results from a basin modeling study, GeoArabia 9 (2004) 41–72.
- [5] T.K. Al-Ameri, A.J. Al-Khafaji, J. Zumberge, Petroleum system analysis of the Mishrif reservoir in Ratawi, Zubair, North and South Rumaila oil fields, southern Iraq, GeoArabia 14 (2009) 91–108.
- [6] Q. Abeed, A.J. Al-Khafaji, R. Littke, Source rock potential of the Upper Jurassic Lower Cretaceous succession in the southern part of the Mesopotamian Basin (Zubair subzone), southern Iraq, J. Pet. Geol. 34 (2011) 117–134.
- [7] A.A.M. Aqrabi, J.C. Goff, A.D. Horbury, F.N. Sadooni, The Petroleum Geology of Iraq, Beaconsfield, United Kingdom: Scientific Press Ltd, PO Box 21, Beaconsfield, Bucks, HP9 1NS, UK, 2010.
- [8] A.S. Al-Sharhan, Albian clastics in the western Arabian Gulf region: a sedimentological and petroleum geological interpretation, J. Pet. Geol. 17 (1994) 279–300.
- [9] A.S. Al-Sharhan, Facies variations, diagenesis and exploration potential of the Cretaceous rudist-bearing carbonates of the Arabian Gulf, Am. Assoc. Pet. Geol. Bull. 79 (1995) 531–550.
- [10] A.S. Al-Sharhan, A.E.M. Nairn, Sedimentary Basins and Petroleum Geology of the Middle East, Elsevier Science B.V, Amsterdam, 1997, p. 843.
- [11] Q. Abeed, D. Leythaeuser, R. Littke, Geochemistry, origin and correlation of crude oils in Lower Cretaceous sedimentary sequences of the southern Mesopotamian Basin, southern Iraq, Org. Geochem. 46 (2012) 113–126.
- [12] van Bellen, R.C. Van, H.V. Dunnington, R. Wetzel, D.M. Morton, Lexique Stratigraphique International, vol. III, Asie, Fascicule 10a Iraq, 1959, 333 pages (Centre National de la Recherche Scientifique).
- [13] T.K. Al-Ameri, F.S. Al-Musawi, D.J. Batten, Palynofacies indications of depositional environments and source potential for hydrocarbons: uppermost Jurassic-Basal Cretaceous Sulaiy Formation, Southern Iraq, Cretac. Res. 20 (1999) 359–363.
- [14] F.H.A. Abdullah, A preliminary evaluation of Jurassic source rock potential in Kuwait, J. Pet. Geol. 24 (2001) 361–378.
- [15] J. Goff, F.A. Al-Medhadi, H.N. Al-Ajmi, N.K. Verma, A.J. Barwise, T.D. Needham, J. M. Henton, N. Neilson, The Jurassic Najmah/Sargelu petroleum system of West Kuwait: a producing fractured carbonate source rock reservoir, in: 6th Middle East Geosciences Conference, GEO 2004. GeoArabia, Abstract, vol. 9, no. 1, 2004, p. 70–71.
- [16] T.K. Al-Ameri, J. Zumberge, Middle and Upper Jurassic hydrocarbon potential of the Zagros Fold Belt, North Iraq, Mar. Pet. Geol. 36 (2012) 13–34.
- [17] J. Hunt, Petroleum Geochemistry and Geology, W.H. Freeman and Company, New York, USA, 1996, p. 743.
- [18] D.K. Baskin, K.E. Peters, Early generation and characteristics of a sulfur-rich Monterey kerogen, Am. Assoc. Pet. Geol. Bull. 76 (1992) 1–13.
- [19] J.A. Gransch, J. Posthuma, On the origin of sulfur in crudes, in: B. Tissot, F. Bienner (Eds.), Advances of Organic Geochemistry, Editions Technip, Paris, 1973, pp. 727–739.
- [20] J.M. Moldowan, P. Sundararaman, M. Schoell, Sensitivity of biomarker properties to depositional environment and/or source input in the Lower Toarcian of S.W., Germany, Org. Geochem. 10 (1985) 915–926.
- [21] H. Huang, M.J. Pearson, Source rock palaeoenvironments and controls on the distribution of dibenzothiophenes in lacustrine crude oils, Bohai Bay Basin, Eastern China, Org. Geochem. 30 (1999) 1455–1470.
- [22] K.E. Peters, C.C. Walters, J.M. Moldowan, The Biomarker Guide: Biomarkers and Isotopes in Petroleum Exploration and Earth History, second ed., vol. 2, Cambridge University Press, Cambridge, 2005.
- [23] B.P. Tissot, D.H. Welte, Petroleum Formation and Occurrence, second ed., Springer Verlag, Berlin, 1984, p. 699.
- [24] M.D. Lawan, Factors controlling the proportionality of vanadium to nickel in crude oils, Geochem. Cosmochim. Acta 48 (1984) 2231–2238.
- [25] H.D. Hedberg, Significance of high-wax oil with respect to genesis of petroleum, Am. Assoc. Pet. Geol. Bull. 52 (1968) 736–750.
- [26] A.J.G. Barwise, Role of nickel and vanadium in petroleum classification, Energy Fuels 4 (1990) 647.
- [27] L.M. Wenger, C.L. Davis, G.H. Isaksen, Multiple controls on petroleum biodegradation and impact on oil quality, Reserv. Eval. Eng. (2002) 375–383.
- [28] Z. Sofer, Stable carbon isotope compositions of crude oils: application to source depositional environments and petroleum alteration, Am. Assoc. Pet. Geol. Bull. 68 (1984) 31–49.
- [29] R.E. Summons, J. Thomas, J.R. Maxwell, C.J. Boreham, Secular and environmental constraints on the occurrence of dinosterane in sediments, Geochem. Cosmochim. Acta 56 (1992) 2437–2444.
- [30] J.W. Collister, D.A. Wavrek, 13C compositions of saturate and aromatic fractions of lacustrine oils and bitumens: evidence for water column stratification, Org. Geochem. 24 (1996) 913–920.

- [31] C.J. Boreham, J.M. Hope, B. Hartung-Kagi, Understanding source, distribution and preservation of Australian natural gas: a geochemical perspective, *Australian Prod. Pet. Explorat. Assoc. J.* 41 (2001) 523–547.
- [32] R.P. Philp, Biological markers in fossil fuel production, *Mass Spectrom. Rev.* 4 (1985) 1–54.
- [33] J.P. Clark, R.P. Philp, Geochemical characterization of evaporate and carbonate depositional environments and correlation of associated crude oils in the Black Creek Basin, Alberta, *Bull. Can. Pet. Geol.* 37 (1989) 401–416.
- [34] D.E. Müller, A.G. Holba, W.B. Huges, Effects of biodegradation on crude oils, in: R.F. Meyer, (Ed.), *Exploration for Heavy Crude Oil and Natural Bitumen*. American Association of Petroleum Geologists Studies, 1987, pp. 233–241.
- [35] G. Rheinheimer, *Aquatic Microbiology*, Wiley, London, 1984, p. 1973.
- [36] S.R. Larter, I.M. Head, H. Huang, B. Bennett, M. Jones, A.C. Aplin, A. Murray, M. Erdmann, A. Wilhelms, R. di Primio, Biodegradation, Gas Destruction and Methane Generation in Deep Subsurface Petroleum Reservoirs: An Overview, in: A.G. Dore, B. Vining (Eds.), *Petroleum Geology: Northwest Europe and Global Perspectives: Proceedings of the 6th Petroleum Geology Conference*, Geological Society, London, 2005, pp. 633–640.
- [37] G. Eglinton, R.G. Hamilton, Leaf epicuticular waxes, *Science* 156 (1967) 1322–1344.
- [38] E. Gelpi, H. Schneider, J. Mann, J. Oró, Hydrocarbons of geochemical significance in microscopic algae, *Phytochemistry* 9 (1970) 603–612.
- [39] P.A. Cranwell, Organic geochemistry of Cam Loch (Sutherland) sediments, *Chem. Geol.* 20 (1977) 205–221.
- [40] S.C. Brassell, G. Eglinton, J.R. Maxwell, R.P. Philp, Natural background of alkanes in the aquatic environment, in: O. Hutzinger, L.H. van Lelyveld, B.C.J. Zoeteman (Eds.), *Aquatic Pollutants: Transformation and Biological Effects*, Pergamon, Oxford, 1978, pp. 69–86.
- [41] T.G. Powell, D.M. McKirdy, Relationship between ratio of pristane to phytane, crude oil composition and geological environment in Australia, *Nature* 243 (1973) 37–39.
- [42] B.M. Didyk, B.R.T. Simoneit, S.C. Brassell, G. Eglinton, Organic geochemical indicators of palaeoenvironmental conditions of sedimentation, *Nature* 272 (1978) 216–222.
- [43] K. Chandra, C.S. Mishra, U. Samanta, A. Gupta, K.L. Mehrotra, Correlation of different maturity parameters in the Ahmedabad-Mehsana Block of the Cambay Basin, *Org. Geochem.* 21 (1994) 313–321.
- [44] K.E. Peters, J.M. Moldowan, *The Biomarker Guide: Interpreting Molecular Fossils in Petroleum and Ancient Sediments*, Prentice-Hall, Inc., Englewood Cliffs, New Jersey, 1993.
- [45] H.L. ten Haven, M. Rohmer, J. Rullkotter, P. Bissere, Tetrahymanol, the most likely precursor of gammacerane, occurs ubiquitously in marine sediments, *Geochim. Cosmochim. Acta* 53 (1989) 3073–3079.
- [46] J.S. Sinninghe Damsté, F. Kenig, M.P. Koopmans, J. Koster, S. Schouten, J.M. Hayes, J.W. de Leeuw, Evidence for gammacerane as an indicator of water column stratification, *Geochim. Cosmochim. Acta* 59 (1995) 1895–1900.
- [47] W.Y. Huang, W.G. Meinschein, Sterols as ecological indicators, *Geochim. Cosmochim. Acta* 43 (1979) 739–745.
- [48] W.K. Seifert, J.M. Moldowan, Application of steranes, terpanes and monoaromatic to the maturation, migration and source of crude oils, *Geochim. Cosmochim. Acta* 42 (1978) 77–95.
- [49] W.K. Seifert, J.M. Moldowan, Palaeoreconstruction by biological markers, *Geochim. Cosmochim. Acta* 45 (1981) 783–794.
- [50] W.K. Seifert, J.M. Moldowan, Use of biological markers in petroleum exploration, in: R.B. Johns (Ed), vol. 24, *Methods in Geochemistry and Geophysics Book Series*, Amsterdam, 1986., pp. 261–90.
- [51] M.I. Roushdy, M.M. El Nady, Y.M. Mostafa, N.S. El Gendy, H.R. Ali, Biomarkers characteristics of crude oils from some oilfields in the Gulf of Suez, Egypt, *J. Am. Sci.* 6 (2010) 911–925.
- [52] M.M. El Nady, F.M. Harb, N.S. Mohamed, Biomarker characteristics of crude oils from Ashrafi and GH oilfields in the Gulf of Suez, Egypt: an implication to source input and paleoenvironmental assessments, *Egypt. J. Petrol.* 23 (2014) 455–459.
- [53] M.S. El-Gayar, A.R. Mostafa, A.E. Abdelfattah, A.O. Barakat, Application of geochemical parameters for classification of crude oils from Egypt into source related types, *Fuel Process. Technol.* 79 (2002) 13–28.